第 48 卷第 1 期　　硅　酸　盐　学　报　　Vol. 48，No. 1
2020 年 1 月　　JOURNAL OF THE CHINESE CERAMIC SOCIETY　　January，2020
http://www.gxyb.cbpt.cnki.net　　**DOI**：10.14062/j.issn.0454-5648.20190231

中红外热熔激光陶瓷粉体制备与性能表征

张学建[1,2]，夏晨阳[1,2]，张守丰[1,2]，李　春[3]，刘卉昇[1,2]，李永涛[1,2]，杨益民[1]，杜傲宸[1]

(1. 吉林建筑大学，长春 130018；2. 长春市结构与功能陶瓷工程研究中心，长春 130018；
3. 长春理工大学材料科学与工程学院，长春 130022)

摘　要：通过溶胶–凝胶法合成 Tm，Ho:$Gd_3Ga_5O_{12}$(Tm, Ho:GGG)纳米粉体，以 $Ga(NO_3)_3$ 和 $Gd(NO_3)_3$ 为原料，并用一定量的 Tm 和 Ho 取代 Gd，合成了 Tm，Ho:GGG 超细粉体。借助 X 射线衍射、红外光谱、扫描电子显微镜、热重分析及荧光光谱技术分析了 Tm，Ho:GGG 超细粉的相结构，热稳定性，粒径和形貌。结果表明：Tm，Ho:GGG 在 900 ℃煅烧后获得粒径均匀，分散性和流动性好的 GGG 纯相纳米粉末，尺寸在 70~90 nm 之间。荧光发射的最强峰位于 1 950 nm，是由 Ho^{3+}的 $^5I_7\rightarrow{}^5I_8$ 转变产生。

关键词：钆镓石榴石；镧系掺杂；纳米粉体
中图分类号：TQ174.5　　**文献标志码**：A　　**文章编号**：0454–5648(2020)01–0061–04
网络出版时间：2019–09–03



Preparation and Characterization of Mid-infrared Hot-melt Laser Ceramic Powders

ZHANG Xuejian[1,2], *XIA Chenyang*[1,2], *ZHANG Shoufeng*[1,2], *LI Chun*[3],*LIU Huisheng*[1,2], *LI Yongtao*[1,2], *YANG Yimin*[1], *DU Aochen*[1]
(1. Jilin Jianzhu University, Changchun 130118, China;
2. Changchun Structural and Functional Material Engineering Research Center, Changchun 130118, China;
3. School of Materials Science and Engineering, Changchun University of Science and Technology, Changchun 130022, China)

Abstract: Tm, Ho:$Gd_3Ga_5O_{12}$ (Tm, Ho:GGG) nanopowders were synthesized *via* the sol–gel method. Tm, Ho:GGG ultrafine powders were synthesized by using $Ga(NO_3)_3$ and $Gd(NO_3)_3$ as raw materials and by replacing Gd with certain amounts of Tm and Ho. The phase structure, thermal stability, particle size, and morphology of the Tm, Ho:GGG ultrafine powers were analyzed by X-ray diffraction, infrared spectroscopy, scanning electron microscopy, thermogravimetry-differential thermal analysis, and fluorescence spectroscopy. The results revealed that a pure GGG phase was obtained after the calcination of Tm, Ho:GGG at 900 ℃, and the obtained nanopowder had a uniform particle size of 70–90 nm, good dispersibility, and fluidity. The fluorescence analysis determined that the strongest peak of the fluorescence emission spectrum was at 1 950 nm, which was associated with the $^5I_7\rightarrow{}^5I_8$ transition of Ho^{3+}.

Keywords: gadolinium gallium garnet; lanthanide doping; nanopowder

1　Introduction

Gadolinium gallium garnet ($Gd_3Ga_5O_{12}$, GGG) has a cubic crystal structure and belongs to the O_h(10)-la 3*d* space group. The properties of GGG are comparable to those of yttrium aluminum garnet (YAG), which is a stable and high-quality laser material[1]. Rare earth luminescent materials have come to attract considerable attention because of their properties and applications[2]. Rare earth luminescent materials are generally classified into four types: powder materials, single-crystal materials, ceramic materials, and glass materials. The powder materials have the widest application scope[3–4]. A series of studies have been conducted to increase the

收稿日期：2019–04–11。　修订日期：2019–05–20。
基金项目：吉林省自然科学基金(20170101090JC)；吉林省产业技术研究与开发项目(2018C042-4)。
第一作者：张学建(1975—)，男，博士，教授。

Received date: 2019–04–11.　**Revised date:** 2019–05–20.
First author: ZHANG Xuejian (1975–), male, Ph.D., Professor.
E-mail: 357169750@qq.com

luminescence intensity of the materials. It has been found that many rare earth ions have abundant energy levels and 4*f* electronic transition characteristics [5]. Tm^{3+}- and Ho^{3+}-doped GGG crystal is a widely used laser material with excellent laser performance that plays an increasingly important role in the field of high-power all-solid-state lasers. Lawrence Livermore Laboratory has selected the GGG crystal as a laser material for the 100 kW short-range solid-state laser[6].

Currently, research on laser ceramics is mainly concentrated on cubic systems such as GGG, YAG, and yttrium gallium garnet (YGG). Among these laser materials, GGG possesses excellent mechanical properties, thermal properties, and optical properties, and it is a good luminescent matrix material. To prepare Tm, Ho:GGG transparent ceramic materials with good light transmittance, it is necessary to first obtain powders with a uniform particle size, high chemical purity, and good dispersibility. At present, commonly used synthesis methods include the solid-state method, wet chemical coprecipitation method, sol–gel method, and hydrothermal method[7–9]. In 2011, Kostyk et al. [10] prepared GGG powders by coprecipitation and provided a good theoretical basis for later researchers. The sol–gel method has the advantages of a low preparation cost, simple preparation process, and short preparation period. Therefore, in this study, Tm, Ho:GGG transparent ceramic precursors with good performance were prepared *via* the sol–gel method by using metal nitrates as raw materials[11]. The structure and morphology of the Tm, Ho:GGG were then characterized.

2 Experimental

2.1 Preparation of Tm, Ho:GGG ultrafine powders

Tm, Ho:GGG ultrafine powders were prepared *via* the sol–gel method by using citric acid as a combustion agent. First, the amounts of the Tm_2O_3, Ho_2O_3, $Ga(NO_3)_3$, and $Gd(NO_3)_3$ raw materials were accurately calculated and weighed according to the molar ratio of $Tm_{0.3}Ho_{0.3}Gd_{2.4}Ga_5O_{12}$. Tm_2O_3 and Ho_2O_3 were each dissolved in 5 mol/L nitric acid to obtain clear colorless acidic solutions, and $Ga(NO_3)_3$ and $Gd(NO_3)_3$ were each dissolved in deionized water to obtain clear colorless acidic solutions. The above four solutions were then uniformly mixed to obtain a mixed nitrate solution containing 1 mol/L trivalent metal cations. Then, a citric acid solution was prepared with a ratio of 1.5 mol of citric acid per mol of total metal ions (Tm, Ho, Gd, and Ga) and added to the nitrate solution to obtain a clear mixed solution. The pH value of the solution was adjusted to 1.5–2.0 by ammonia titration to decrease the oxidizability and to obtain the mother solution. Next, the solution was stirred and heated at 60 ℃ for 3 h to obtain a transparent gel. The gel was transferred to an oven at 200 ℃, where it remained for 2 h. During this time, the transparent gel expanded and filled the entire container, while the bottom of the gel burned and generated a large amount of brown gas. Finally, a black dry gel was obtained. After grinding, the black dry gel was divided into 3 parts that were calcined at 800, 900, and 1 000 ℃.

2.2 Test method

The calcined powders were characterized by X-ray diffraction (XRD) on a D/max-RA instrument (Rigaku, Japan), using Cu K_α radiation and a graphite monochromator at 50 kV and 150 mA. The precursor was subjected to thermogravimetry-differential thermal analysis (TG–DTA) using a simultaneous thermal analysis (STA) instrument (Model SDT2960, TA Instruments, USA). The heating rate was 10 ℃/min, and the air flow rate was 10 mL/min. The microstructure, particle size, and agglomeration of the powder were characterized by scanning electron microscopy (SEM, Model JXA-840, JEOL Ltd., Japan). Infrared (IR) spectra of the sample were acquired by BIO-RAD FTS135 Fourier transform infrared spectroscopy (USA, resolution 4 cm^{-1}, in the range of 4 250–250 cm^{-1}) using KBr tablet method. The fluorescence spectrum of the ceramic precursor was obtained on a photoluminescence fluorescence spectrometer (PFS, Model PL9000, Philips, Netherland) with an excitation wavelength of 980 nm by Ar ions.

3 Results and discussion

3.1 XRD analysis

The XRD patterns of the Tm, Ho:GGG prepared by the sol–gel method at the different calcination temperatures are shown in Fig. 1. After the 800 ℃ calcination, the characteristic diffraction peaks of the Tm, Ho:GGG phase appear, which indicates that a microcrystalline phase of Tm, Ho:GGG was formed at this temperature. Compared with the standard PDF of Tm, Ho:GGG, however, the peaks of the 800 ℃ calcined Tm, Ho:GGG are not only less sharp but also accompanied by miscellaneous phases and peak shifts. For the 900 ℃ calcined sample, each diffraction peak corresponds to a characteristic diffraction peak of the Tm, Ho:GGG phase. The peak intensity of the 900 ℃ calcined sample is greatly increased compared with that of the 800 ℃ calcined sample. The peak position does not change significantly as the calcination temperature increases. The result shows that the Ga^{3+} and Gd^{3+} in the precursor powder were uniformly mixed at the ion level. A precursor powder with Gd^{3+}:Ga^{3+}=3:5 was formed, and a Tm, Ho:GGG phase was directly formed by calcination.

It can be seen from Fig. 1 that as the calcination temperature increases, the intensity of the diffraction peaks gradually increases while the half-width of the peaks decreases. According to the Scherrer equation:

$$D=0.89\lambda/B\cos\theta \quad (1)$$

Where D is the average thickness of grains perpendicular to the crystal plane; λ is X-ray wavelength; B is the half-height width of the diffraction peak of measured sample; θ is diffraction angle. The particle size of the powder increases as the calcination temperature increases. To meet the particle size requirement for raw

crystal materials, the optimum calcination temperature for synthesizing the Tm, Ho:GGG polycrystalline phase was determined to be 900 ℃.

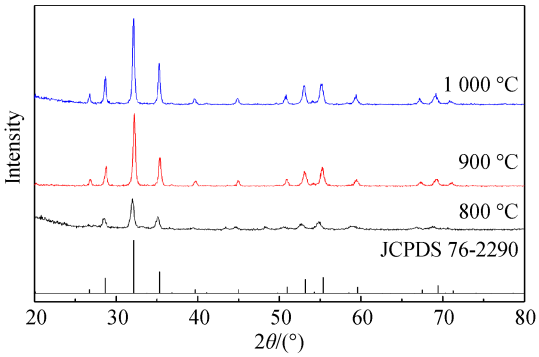


Fig. 1　XRD patterns of Tm, Ho:GGG samples prepared by the sol–gel method and calcined at different temperatures for 4 h

3.2　IR analysis

The molecular structure and chemical composition of the Tm, Ho:GGG ultrafine powder after the 900 ℃ calcination were qualitatively analyzed by IR spectroscopy. The IR spectrum of the precursor is shown in Fig. 2. The absorption band at 3 580 cm^{-1} is attributed to the overlap of the (O–H) bond in the adsorbed H_2O, the asymmetric stretching vibration of the hydrogen bond, and the CH_2 group. The absorption band at 1 478 cm^{-1} is attributed to the bending vibration of the (O–H) bond in H_2O. As the temperature increases, the areas and intensities of both bands decrease, which indicates that the water content decreases. The absorption band at 1 593 cm^{-1} is attributed to the overlap of the vibration absorption bands of various C=O bonds attached to different groups (CH, OH, Cl, NH_2, *etc*.). The weak absorption band at 1 184 cm^{-1} is attributed to a small amount of CO_3^{2-}. The absorption peaks at 691 and 915 cm^{-1} indicate the presence of small amounts of substituent groups such as Cl and NH_2. The IR spectrum of the 900 ℃ calcined powder is shown in Fig. 3. The weak absorption peak at 3 452 cm^{-1} is attributed to the small amount of H_2O that is adsorbed on the powder in air. The absorption peaks at 690, 658, and 582 cm^{-1} correspond to the Gd–O polyhedron, Gd–O–Ga bond, *etc*., which indicates the formation of the GGG phase. In addition, these absorption peaks are sharp and distinct, which suggests that the crystallization of the GGG phase tends to be perfect.

3.3　TG–DTA analysis

The TG–DTA curve of the precursor is shown in Fig. 4. The TG curve shows that the mass loss of the sample is a continuous process, and the total mass loss is 39.24 %. The endothermic peak at 106 ℃ is associated with the evaporation of adsorbed water and free water. The main mass loss of 21.34 % occurs from 95–208 ℃, which is caused by the oxidation of organics. The mass loss of 5.34% at 470–803 ℃ is caused by the removal of CO_2 that is adsorbed on the particle surface. The exothermic peaks in the DTA curve are attributed to the oxidation and decomposition of the organics. A weak exothermic peak appears near 873 ℃, while the sample mass loss is minimal. The result indicates a phase transition at this temperature. The exothermic peak is caused by the primary crystallization of $Ga(NO_3)_3$ and $Gd(NO_3)_3$ to form polycrystalline GGG.

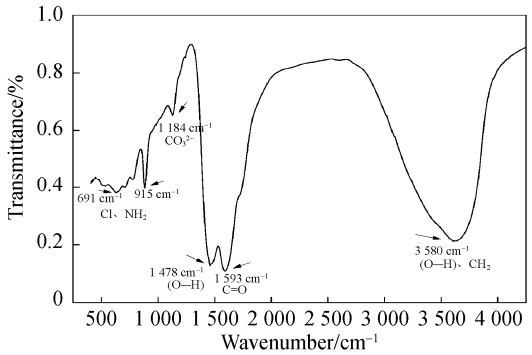


Fig. 2　IR spectrum of the precursor

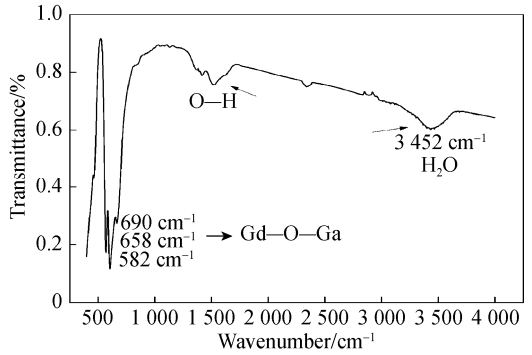


Fig. 3　IR spectrum of the calcined powder

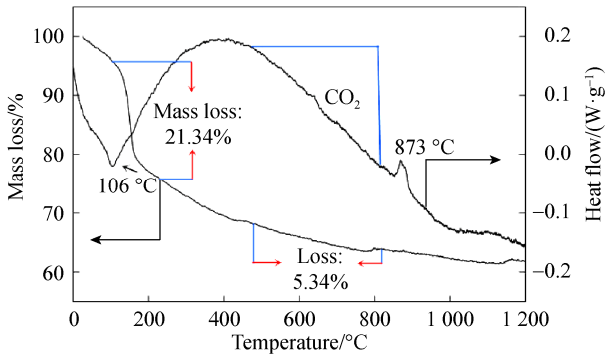


Fig. 4　TG–DTA curves of the precursor

3.4　SEM analysis

The concentration of the solution, the combustion agent, and the temperature all have influences on the preparation of the Tm, Ho:GGG ultrafine powder by the sol–gel method. In this study, an SEM analysis of Tm, Ho:GGG ultrafine powders calcined at different temperatures including 800, 900, and 1 000 ℃ was carried out. The results show that the powder obtained by calcination at 800 ℃ is observed to exhibit a nonuniform particle size and excess impurities. As the temperature increases to 1 000 ℃, the powder becomes severely

agglomerated, and the dispersibility is poor. The above factors were considered comprehensively based on the experimental results. The SEM morphology of the Tm, Ho:GGG sample calcined at 900 ℃ is shown in Fig. 5. The particles are spherical/spheroidal and uniformly dispersed, and the particle size is relatively uniform, generally 70–90 nm.

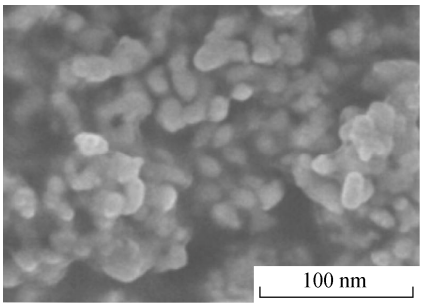


Fig. 5 SEM morphology of the Tm, Ho:GGG powder after calcination at 900 ℃

3.5 Fluorescence spectroscopy

The fluorescence spectrum of the powder sample in the range of 1 600–2 000 nm measured by a 980 nm excitation source at room temperature is shown in Fig. 6. A series of emission peaks were observed in this range, and the strongest emission peak is located at 1 950 nm. The energy transfer diagram of the Tm, Ho:GGG nanopowder excited at 980 nm is shown in Fig. 7. After absorbing the 980 nm laser radiation, Tm^{3+} ions were excited from the ground state $^3H_6$ into the excited state $^3F_3$. Then, the $^3F_4$ energy level was populated *via* a cross-relaxation mechanism through the following process.

$$^3F_3 + {}^3H_6 \rightarrow {}^3F_4 + {}^3F_4 \quad (2)$$

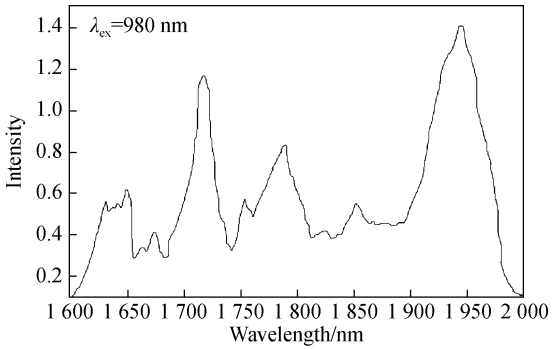


Fig. 6 Fluorescence spectrum of the Tm, Ho:GGG powder

The $^3F_4$ energy level of Tm^{3+} is very close to the $^5I_7$ energy level of Ho^{3+}. Hence, cross-relaxation and resonant energy transfer can occur between the Tm^{3+} in $^3F_4$ and the Ho^{3+} in $^5I_7$. The Tm^{3+} $^3F_4$ and Ho^{3+} $^5I_7$ energy levels are dynamically balanced during this process. Finally, a radiation transition of Ho^{3+} from $^5I_7$ to the ground state $^5I_8$ is achieved, which contributes to the 1.95 μm fluorescence emission. As evidenced by the fluorescence test of the GGG powder doped with two rare earth elements, the sample generates a fully stable light, which proves that GGG is a completely stable structure.

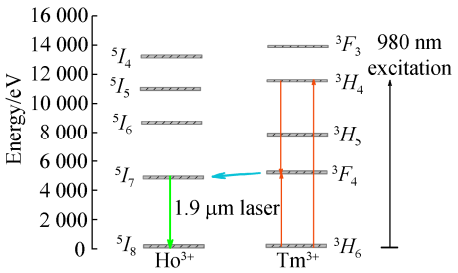


Fig. 7 Energy level diagram of Tm^{3+} and Ho^{3+} of the Tm, Ho:GGG powder

4 Conclusion

1) The as-prepared Tm, Ho:GGG powder had crystallized before calcination. A pure Tm, Ho:GGG phase was formed at a calcination temperature of 900 ℃.

2) The Tm, Ho:GGG polycrystalline nanopowder had a uniform particle size of approximately 50–70 nm and good dispersibility.

3) The strongest fluorescence emission peak of the Tm, Ho:GGG polycrystalline nanopowder was at 1 950 nm, which was associated with the $^5I_7 \rightarrow {}^5I_8$ transition of Ho^{3+}.

References:

[1] JIANG B, ZHAO Z, XU J, et al. Room temperature absorption and emission spectra of Nd^{3+}:$Gd_3Ga_5O_{12}$ crystals[J]. J Synth Cryst, 2004, 33(4): 581–585.

[2] KIM S-G, SHIN D-W, KIM T, et al. Large-scale freestanding nanometer-thick graphite pellicles for mass production of nano devices beyond 10 nm[J]. Nanoscale, 2015, 7: 14608–14611.

[3] ZHANG S. Rare earth ion spectroscopy[M]. Beijing: Science Press, 2008: 13–14.

[4] HONG G. Research progress of rare earth luminescent materials[J]. J Synth Cryst, 2015, 44(10): 2641–2650.

[5] LI Y, LU H, ZHANG Y, et al. Synthesis and luminescence properties of $Gd_3Ga_5O_{12}$:Eu^{3+} nanocrystals by citric acid combustion method[J]. J Synth Cryst, 2012, 41(4): 911–915.

[6] ZHANG Q, YIN S, WANG A, et al. Research progress of the laser crystal GGG species[J]. Chin J Quantum Electron, 2002, 19(6): 481–484.

[7] LI J, IKEGAMI T, LEE J-H, et al. Co-precipitation synthesis and sintering of yttrium aluminum garnet (YAG) powders: The effect of precipitant[J]. J Eur ceram Soc, 2000, 20: 2395–2045.

[8] WEN L, SUN X, MA W. Fabrication of transparent Nd:YAG ceramics by a solid-state reaction method [J]. J Inorg Mater, 2004, 19(2): 295–301.

[9] HAKUTA Y, SEINO K, URA H, et al. Production of phosphor (YAG:Tb) fine particles by hydrothermal synthesis in supercritical water[J]. J Mater Chem, 1999, 9: 2671–2674.

[10] KOSTYK L, LUCHECHKO A, VARVARENKO S, et al. Preparation and luminescence properties of $Ga_3Gd_5O_{12}$ nanocrystalline garnet[J]. Chem Met Alloy, 2011, 4: 77–80.

[11] JIANG L, SUN J, ZENG F, et al. Properties and preparation of Cr, Nd:GGG laser ceramic raw materials[J]. J Chin Soc Rare Earth, 2014, 32(2): 177–181.